DINAME 2017 - Proceedings of the XVII International Symposium on Dynamic Problems of Mechanics
A. T. Fleury, D. A. Rade, P. R. G. Kurka (Editors), ABCM, São Sebastião, SP, Brazil, March 5-10, 2017

NONLINEAR IDENTIFICATION USING POLYNOMIAL NARMAX MODEL AND A STABILITY ANALYSIS OF AN AEROELASTIC SYSTEM

Raphaela Carvalho Machado Gonçalves Barbosa [1], **Luiz Carlos Sandoval Góes**[1], **Airton Nabarrete**[1], **Jose Manoel Balthazar**[1], **David Fernando Castillo Zúñiga**[1]

[1] Instituto Tecnológico de Aeronáutica - ITA, Praça Marechal Eduardo Gomes, 50 - São José dos Campos, 12228-900, Brazil. e-mail: machado@ita.br, goes@ita.br, nabarrete@ita.br, jmbaltha@ita.br, davidfer@ita.br

Abstract: This work describes the nonlinear identification applied to an aeroelastic pitch-plunge system using polynomial NARMAX model and a stability analysis. The apparatus is available and consists of a wing typical section with pitch and plunge degrees of freedom. The rigid wing has one flight control surface and is supported by an elastic structure with low damping. The identification procedure aims to obtain the parameters for the mathematical model incorporating the nonlinearity to the support torsional stiffness as a quadratic polynomial function. The candidate structure to the polynomial NARMAX model is obtained from discretization of the continuous-time state-space model that has been derived from the governing equation of motion of the aeroelastic system considering two degrees of freedom. Theoretical continuous-time model parameters and equation coefficients relationship are presented. The predictions for the theoretical discrete-time model are obtained via the identification procedure using polynomial NARMAX model with data from the simulated model. This simulation is performed considering the aerodynamics promoted by wind tunnel with free stream velocity increased within an established velocity range which includes the flutter phenomenon. In future work, the nonlinear identification using the experimental data acquisition from the experimental apparatus will be performed. The polynomial NARMAX model indicates a polynomial function of fourth order for representing the nonlinear torsional stiffness of the dynamic system. The stability analysis is also discussed in this work and a mapping with nonlinear regions is shown.

Keywords: nonlinear system identification, polynomial NARMAX model, aeroelastic system, stability analysis.

NOMENCLATURE

m_T: total mass.
I_α: mass moment of inertia.
a: nondimensional distance from the midchord to the elastic axis (e.a.).
b: semichord of the wing.
x_α: distance between the e.a. and the c.g.
c_h, c_α: viscous damping coefficient.
k_h, k_α: structural stiffness.
ρ: air density.
L: aerodynamic lift.
M: aerodynamic moment.
β: control surface.
V_∞: free stream velocity.
$C_{l\alpha}$, $C_{m\alpha}$: lift and moment coefficient per angle of attack.
$C_{l\beta}$, $C_{m\beta}$: lift and moment coefficient per angle of the control surface.
k_{α_0}, k_{α_1}, k_{α_2}, k_{α_3}, k_{α_4}: coefficients of torsional stiffness.
t: time
n: multiple of sample period.
$h(t)$: linear displacement.
$\alpha(t)$: angular displacement.
$\dot{h}(t)$: linear velocity.
$\dot{\alpha}(t)$: angular velocity.
$\ddot{h}(t)$: linear acceleration.
$\ddot{\alpha}(t)$: angular acceleration.
$\mathbf{x}$(t): vector of generalized displacement.
$\dot{\mathbf{x}}$(t): vector of generalized velocity.
$\boldsymbol{Q}$: lift and moment vector.
$\boldsymbol{M}$: mass matrix.
$\boldsymbol{K}$: stiffness matrix.
$\boldsymbol{C}$: viscous damping matrix.
$\mathbf{J}$: Jacobian matrix.
λ: eigenvalues of the Jacobian matrix.
k: number of iteration.
ξ_k: residue in k iteration.
$\mathbf{y}$: output vector.
$\hat{\mathbf{y}}$: predicted output vector.
$\mathbf{e}$: residue vector.
ψ: regression matrix.
θ: parameter estimate.
$\sigma_{\dot{h}}^2$: covariance of noise related to linear velocity.
$\sigma_{\dot{\alpha}}^2$: covariance of noise related to angular velocity.
σ_{ξ}^2: covariance of residue.
θ_1,...,θ_{10}: discrete-time model parameters for plunge velocity.
γ_1,...,γ_{10}: discrete-time model parameters for pitch velocity.

INTRODUCTION

Recent researches exhibited aeroelastic systems presenting phenomena such as limit cycle oscillation (LCO) occurring due to nonlinearities. Many of these studies demonstrate the aeroelasticity of aircraft wings based on typical section model. O'Neil *et al.* (1996a) reported the output response to an aeroelastic pitch-plunge system in which a polynomial of fifth order modeled the torsional stiffness. In other work O'Neil *et al.* (1996b) demonstrates the LCO caused by the

nonlinearity and considers the free stream velocity as the main parameter to increase oscillations amplitudes. The stiffness nonlinearity is also estimated through the experiments by O'Neil and Strganac (1998), where they proposed an aeroelastic system composed by a rigid wing supported by cubic springs. Indeed, unstable regions associated to LCO are predicted and evidences of internal resonance behavior is verified in the apparatus. Strganac *et al.* (2000) presents the identification of a limit cycle oscillation (LCO) in an aeroelastic system, concluding that sometimes a nonlinear approach is necessary for designing a control system. Based on this research other control strategies are discussed for the suppression of LCO, for instance the nonlinear adaptive controller. More recently Abdelkefi *et al.* (2012) treats on the representation of a freeplay nonlinearity from periodic responses in which a polynomial cubic is estimated. In Xu *et al.* (2015), they report a nonlinear flutter control law based on state variable feedback that is designed to suppress the LCO to an airfoil system with a hysteresis as nonlinearity. Additionally, the effects of a time delay between the control and actuator is investigated showing they cause high-frequency vibrations. A nonlinear analysis and control of aeroelastic systems have been reported by Shukla (2016) where a methodology to generate accurate estimates of LCO amplitude is presented and a controller design from a multi objective optimization problem is employed to eliminate the subcritical LCO.

The researches on nonlinear aeroelastic systems have been stated and the system identification has been performed to identify or adjust the characteristic of the structural nonlinearities (cubic, quadratic, hysteresis or freeplay) using its time history. In this work an identification procedure is applied to the experimental apparatus of a typical section intending the posterior stability analysis based on the model performance. In the model the torsional spring has a nonlinear stiffness that behaves as a fourth order polynomial, and for which the nonlinear effects are investigated in this research. The experimental apparatus is presented in Figure 1. Some methodologies for nonlinear identification are described in the literature. Popescu *et al.* (2005) presents the identification the nonlinearities based on nonparametric estimation. On the other hand, the parametric estimation proposed by Kukreja (2008) is performed using the polynomial NARMAX (nonlinear autoregressive moving average exogenous) to identify the quadratic nonlinearity from the experimental data of an airfoil without control surface. Additionally, Obeid (2012) presented a closed loop feedback control of an airfoil with high angles of attack using a NARMAX model. In this way, the nonlinear model is identified from simulated data using a polynomial NARMAX model to capture the static nonlinearity due to torsional spring. The identified model explains the system behavior, e.g., the flutter phenomenon that causes the limit cycle oscillations, useful to the feedback control system design and the evaluation of the airfoil performance. This procedure will be used in a future work with the experimental data acquisition of the experimental apparatus.

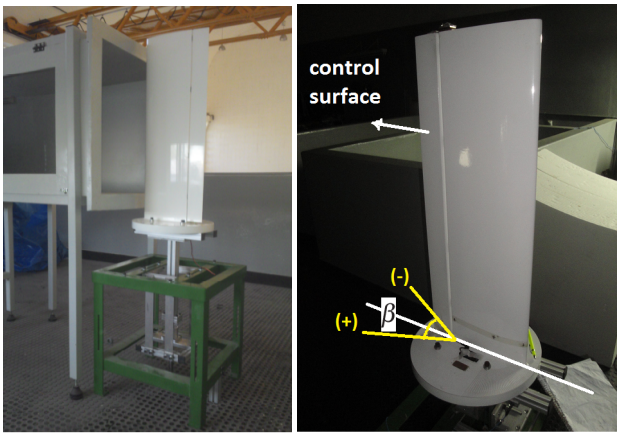

(a) (b)

Figure 1 – Airfoil apparatus available at the Laboratory.

NONLINEAR AEROELASTIC MODEL

The equations of motion of the typical section as depicted in Figure 2 consider two degrees of freedom as functions of time, plunge $h(t)$ and pitch $\alpha(t)$, for the dynamic response of the system. The trailing edge control surface angle β is considered as a control input of the model. The parameters of the dynamic model consist of mass m_T, linear stiffness k_h related to the translation (plunge), moment of inertia I_α and nonlinear torsional stiffness $k_\alpha(\alpha)$ related to the angular displacement of pitch. The inherent damping of the system is modeled as produced exclusively by the deformation of the elastic elements. The damping coefficients are obtained from modal testing. Aerodynamic lift L and moment M are external efforts applied to the dynamic system. Some coefficients are chosen in accordance with experimental apparatus as shown in Table 1 and some others are defined according to O'Neil (1996). The mathematical model of the aeroelastic system is presented as

$$\begin{bmatrix} m_T & m_T x_\alpha b \\ m_T x_\alpha b & I_\alpha \end{bmatrix} \begin{Bmatrix} \ddot{h} \\ \ddot{\alpha} \end{Bmatrix} + \begin{bmatrix} c_h & 0 \\ 0 & c_\alpha \end{bmatrix} \begin{Bmatrix} \dot{h} \\ \dot{\alpha} \end{Bmatrix} + \begin{bmatrix} k_h & 0 \\ 0 & k_\alpha(\alpha) \end{bmatrix} \begin{Bmatrix} h \\ \alpha \end{Bmatrix} = \begin{Bmatrix} -L \\ M \end{Bmatrix} \tag{1}$$

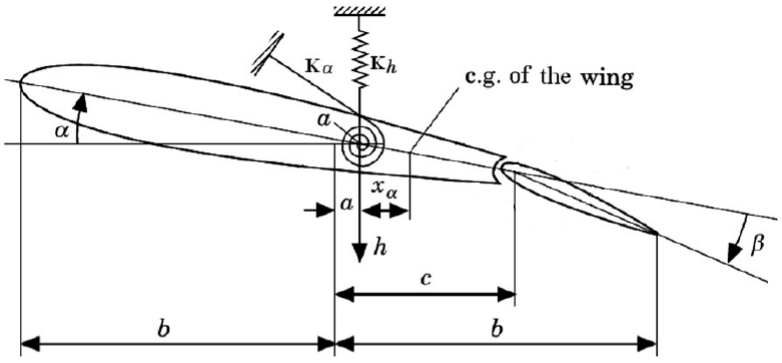

Figure 2 – Typical section model of an airfoil (Li, 2010).

The influence of aerodynamic lift and moment on the airfoil is considered under free stream velocity V_∞. Additionally, the model includes the angular position of the control surface β. With some parameters adopted as referred in Kukreja (2008), the quasi-steady aerodynamic lift and moment are evaluated as

$$L = \rho U^2 b C_{l\alpha}\left[\alpha + \frac{\dot{h}}{U} + \left(\frac{1}{2} - a\right) b\frac{\dot{\alpha}}{U}\right] + \rho U^2 b C_{l\beta}\beta \tag{2}$$

$$M = \rho U^2 b^2 C_{m\alpha}\left[\alpha + \frac{\dot{h}}{U} + \left(\frac{1}{2} - a\right) b\frac{\dot{\alpha}}{U}\right] + \rho U^2 b^2 C_{m\beta}\beta$$

The nonlinear torsional stiffness is modeled as a polynomial of fourth order

$$k_\alpha(\alpha, t) = k_{\alpha_0} + k_{\alpha_1}\alpha + k_{\alpha_2}\alpha^2 + k_{\alpha_3}\alpha^3 + k_{\alpha_4}\alpha^4 \tag{3}$$

Rearranging the terms from Equation 1 the stiffness and damping matrices are obtained including the aeroelastic influence under the free stream velocity as

$$\begin{bmatrix} m_T & m_T x_\alpha b \\ m_T x_\alpha b & I_\alpha \end{bmatrix}\begin{Bmatrix} \ddot{h} \\ \ddot{\alpha} \end{Bmatrix} + \begin{bmatrix} c_h & 0 \\ 0 & c_\alpha \end{bmatrix}\begin{Bmatrix} \dot{h} \\ \dot{\alpha} \end{Bmatrix} + \begin{bmatrix} \rho U b C_{l\alpha} & \rho U b^2 C_{l\alpha}\left(\frac{1}{2} - a\right) \\ \rho U b^2 C_{m\alpha} & -\rho U b^3 C_{m\alpha}\left(\frac{1}{2} - a\right) \end{bmatrix}\begin{Bmatrix} \dot{h} \\ \dot{\alpha} \end{Bmatrix} \tag{4}$$

$$+ \begin{bmatrix} k_h & 0 \\ 0 & k_\alpha(\alpha) \end{bmatrix}\begin{Bmatrix} h \\ \alpha \end{Bmatrix} + \begin{bmatrix} 0 & \rho U^2 b C_{l\alpha} \\ 0 & -\rho U^2 b^2 C_{m\alpha} \end{bmatrix}\begin{Bmatrix} h \\ \alpha \end{Bmatrix} = \begin{bmatrix} -\rho b C_{l\beta} \\ \rho b^2 C_{m\alpha} \end{bmatrix} U^2\beta$$

The constant value of the plunge stiffness and the coefficients of the nonlinear torsional stiffness are informed in the Table 1, in the same way as some other necessary parameters.

Table 1 – Continuous model parameters.

Parameter	Value	Parameter	Value	Parameter	Value
m_T $[kg]$	8	ξ_h	0.022	k_{α_0} $[N\,m/rad]$	3
I_a $[kg\,m^2]$	0.0505	ξ_α	0.03	k_{α_1} $[N\,m/rad^2]$	-30
x_a $[m]$	0.084	c_h $[N\,s/m]$	6.6373	k_{α_2} $[N\,m/rad^3]$	6600
b $[m]$	0.1064	c_α $[N\,s\,m]$	0.2939	k_{α_3} $[N\,m/rad^4]$	-21000
a	-0.8	k_h $[N/m]$	2844.4	k_{α_4} $[N\,m/rad^5]$	48000

The system response is evaluated with constant free stream velocity $V_\infty = 6\ m/s$. The plunge h and pitch α responses are based on their initial conditions. Two upper graphics on Figure 3 show the time history for displacements with the initial conditions $h(0) = 0.1\ m$ and $\alpha(0) = 0.01\ rad$. In these graphics the control surface is located in the neutral angular position, $\beta = 0\ deg$. It is not possible to note the influence of the stiffness nonlinearity considering these responses only. The two graphics below in the same figure show the time history for vertical and angular velocities.

In Figure 3 the nonlinear influence is very difficult to be noted, but it is better observed in Figure 7. After some calculations the angular moment is showed as a function of the angular displacement α, being the static nonlinearity conveniently modeled as $k_\alpha(\alpha) = 3(1 - 10\alpha + 2200\alpha^2 - 7000\alpha^3 + 16000\alpha^4)$. The time history considers also the free stream velocity $V_\infty = 6\ m/s$ and a pitch angle of $-15\ deg$ is outlined as initial condition. The angular displacement is set to $\beta = 15\ deg$, considering it positive or negative, as specified for the maximum nominal angular displacement of the control surface.

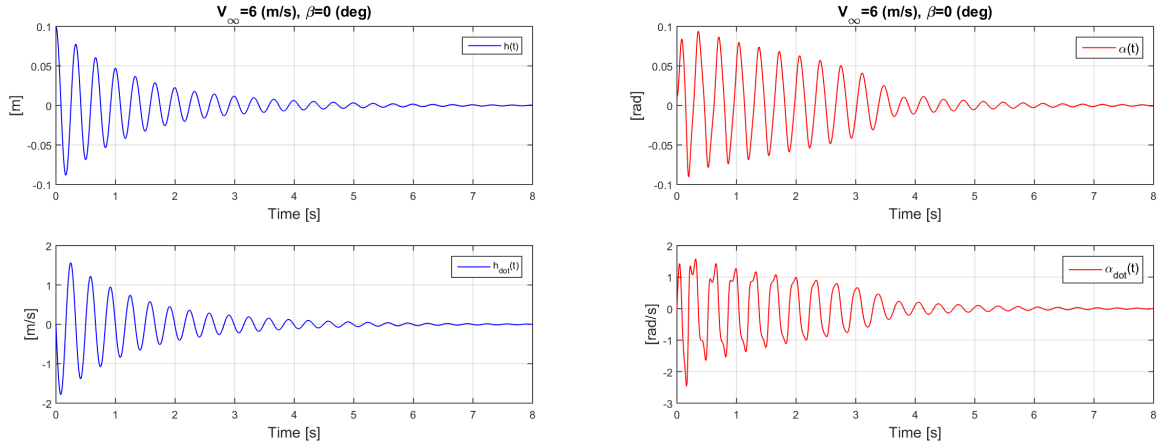

(a) (b)

Figure 3 – Time history for initial conditions $h(0) = 0.1\ m$ and $\alpha(0) = 0.01\ rad$: (a) vertical displacement and velocity; (b) angular displacement and velocity.

NONLINEAR IDENTIFICATION USING POLYNOMIAL NARMAX MODEL

After obtaining the time history from system simulation, the nonlinear identification procedure is applied to obtain a discrete-time model that represents the system dynamics. Firstly, it is presented the selection of the model structure based on discretization of the continuous-time model. After, the nonlinear system identification is performed considering the measurement noise applied to the linear velocity and angular velocity.

System identification using only input-output experimental data allows for a black box model. In this section the nonlinear identification using a polynomial NARMAX model is applied, but the structure selection is in some sense based on the continuous-time model from the previously section. Therefore the known system, narrow box model, is used and a relationship between a continuous-time model and an identified discrete-time model is possible. Finally the model is not totally unknown and a plunge stiffness estimating can be obtained based on the procedure presented in Kukreja (2008).

The nonlinear identification using polynomial NARMAX model consists in the representation of the system output as a polynomial function of $y(n)$, $u(n)$ and $e(n)$ with nonlinearity order l. It follows

$$y(n) = F^l\left[y(n-1),\cdots,y(n-n_y),u(n-n_u-d),\cdots,u(n-n_u),e(n-1),\cdots,e(n-n_e)\right]+e(n) \tag{5}$$

The following section presents the structure obtained to represent the system dynamics. The model structure have two outputs, $\dot{h}(n)$ and $\dot{\alpha}(n)$, with delays $n_y = 1$, $n_u = 1$, $n_e = 1$, dead time $d = 0$, nonlinearity order $l = 5$ corresponding to polynomial of fourth order to represent the torsional stiffness $k_\alpha(\alpha)$. The nonlinear identification deals with a typical least square problem. As so, the nonlinearities appear in the regression matrix and the problem is linear in the parameters. It becomes

$$y(n) = \psi^T(n-1)\hat{\theta} + \xi(n) \tag{6}$$

Model structure selection

The model structure considered to this system is represented by a NARMAX model based in results obtained by Kukreja (2008), whose quadratic stiffness type is described in Ko (1996). In order to describe the model used in the identification process, it is mass-normalized as

$$\ddot{\mathbf{x}} + \mathbf{M}^{-1}\mathbf{C}\dot{\mathbf{x}} + \mathbf{M}^{-1}\mathbf{K}\mathbf{x} = \mathbf{M}^{-1}\mathbf{Q} \tag{7}$$

where, $\ddot{\mathbf{x}} = \begin{Bmatrix} \ddot{h} \\ \ddot{\alpha} \end{Bmatrix}$ and $\mathbf{Q} = \begin{Bmatrix} -L \\ M \end{Bmatrix}$.

Rearranging, the continuous-time model is represented as

$$\begin{Bmatrix} \ddot{h} \\ \ddot{\alpha} \end{Bmatrix} = \begin{Bmatrix} -k_1 h - [k_2\mu + pk_\alpha(\alpha)] - c_1\dot{h} - c_2\dot{\alpha} \\ -k_3 h - [k_4\mu + qk_\alpha(\alpha)] - c_3\dot{h} - c_4\dot{\alpha} \end{Bmatrix} \tag{8}$$

The parameters $\mu = U^2\beta$ and parameters k_1, k_2, k_3, k_4, c_1, c_2, c_3, c_4 are described according to (Kukreja, 2008) and $p = (mx_a b)/b$ and $q = m/d$.

The discrete-time nonlinear model used in the identification procedure is obtained from discretization of Equation 8 by applying the Forward Euler Method given by

$$\dot{h}(n) = \dot{h}(n-1) + T\ddot{h}(n-1) \tag{9}$$

$$\dot{\alpha}(n) = \dot{\alpha}(n-1) + T\ddot{\alpha}(n-1)$$

Note that the variable n is the multiple of sample period. The NARMAX structure follows the discrete-time model represented as

$$\dot{h}(n) = \theta_1\dot{h}(n-1) + \theta_2 h(n-1) + \theta_3\alpha(n-1) + \theta_4\alpha(n-1)^2 + \theta_5\alpha(n-1)^3 + \theta_6\alpha(n-1)^4 + \theta_7\alpha(n-1)^5 \quad (10)$$

$$+\theta_8\dot{\alpha}(n-1) + \theta_9 u(n-1) + \theta_{10}e_{\dot{h}}(n-1) + e_{\dot{h}}(n)$$

$$\dot{\alpha}(n) = \gamma_1\dot{\alpha}(n-1) + \gamma_2 h(n-1) + \gamma_3\alpha(n-1) + \gamma_4\alpha(n-1)^2 + \gamma_5\alpha(n-1)^3 + \gamma_6\alpha(n-1)^4 + \gamma_7\alpha(n-1)^5$$

$$+\gamma_8\dot{h}(n-1) + \gamma_9 u(n-1) + \gamma_{10}e_{\dot{\alpha}}(n-1) + e_{\dot{\alpha}}(n)$$

All parameters used above are shown in Table 2.

Table 2 – Discrete-time model parameters.

Parameter	Value	Identified	Parameter	Value	Identified
θ_1	0.9986	0.9986	γ_1	0.9938	0.9938
θ_2	-0.3601	-0.3601	γ_2	0.5099	0.5105
θ_3	-0.0041	-0.0041	γ_3	-0.0737	-0.0737
θ_4	0.0018	0.0019	γ_4	0.2006	0.2024
θ_5	-0.3944	-0.4060	γ_5	-44.1227	-44.1026
θ_6	1.2548	0.9508	γ_6	140.3904	135.9770
θ_7	-2.8680	21.3053	γ_7	-320.8924	-238.6472
θ_8	-0.0000	-0.0000	γ_8	-0.0011	-0.0011
θ_9	-0.0019	-0.1110	γ_9	-0.0035	-0.2021
θ_{10}	-0.9986	-0.9529	γ_{10}	-0.9938	-0.9515

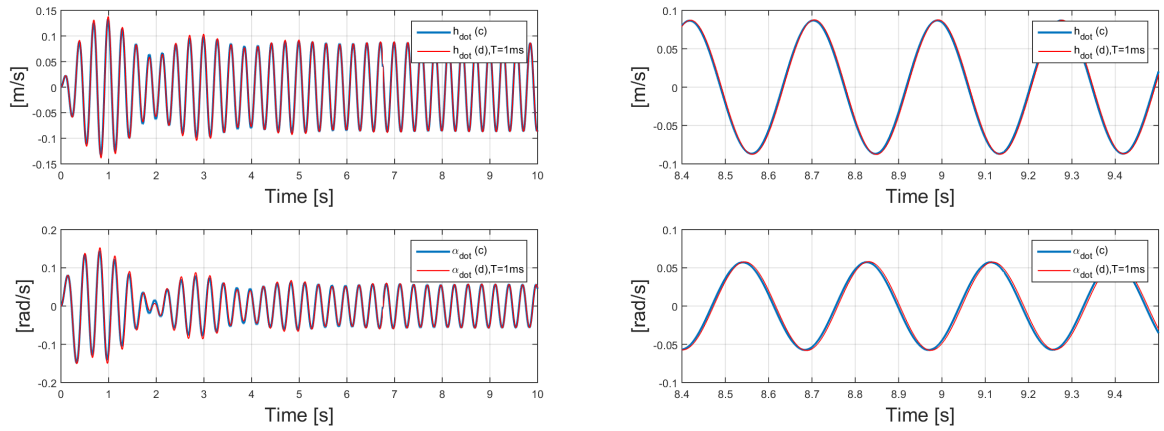

(a) (b)

Figure 4 – (a) Comparison between the continuous-time and discrete-time models and (b) Graphs enlarged in time.

In order to show the performance of the model discretization, null initial conditions, free stream velocity of 6 m/s and harmonic oscillation of the control surface with the frequency of 3.5 Hz are used for graphing the time history as depicted in the Figure 4. The sampling rate of 1 kHz is defined considering the fastest system dynamics and the Nyquist Theorem. In the following the obtained discrete-time model is applied to collect data from the aeroelastic system.

Identification of the system with noise

A polynomial NARMAX model is used to identify the system with noise. The identification procedure consists on the application of an Extended Least Square Estimator (ELS) as indicated by Aguirre (2007), following the sequential steps below:

Step 1. Mount the matricial equation $\mathbf{y} = \psi\theta + \mathbf{e}$ from the measured data to determine $\hat{\theta}_{LS}$.
Step 2. Calculate the residue $\xi_1 = \mathbf{y} - \hat{\mathbf{y}}$.
Step 3. Take $k = 2$;
Step 4. Mount the regression matrix ψ_k^* using the extended regressors from the estimative $\theta_{ELS,k}^*$
Step 5. Calculate the residue $\xi_k = \mathbf{y} - \hat{\mathbf{y}}^*$

Step 6. Take $k = k+1$ and return back to *Step 4*. Repeat until it converges. The criterion for looping stop can be performed using the residue variance $\sigma^2_{\xi_k}$ or the parameters vector $\theta^*_{ELS,k}$. Typically, occurs in the range $3 \leq k \geq 10$.

This procedure basically consists in identifying a NARX model to follow with the construction of a NARMAX structure, including the moving average.

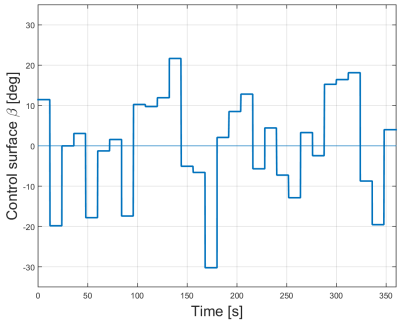

Figure 5 – Excitation signal for system identification.

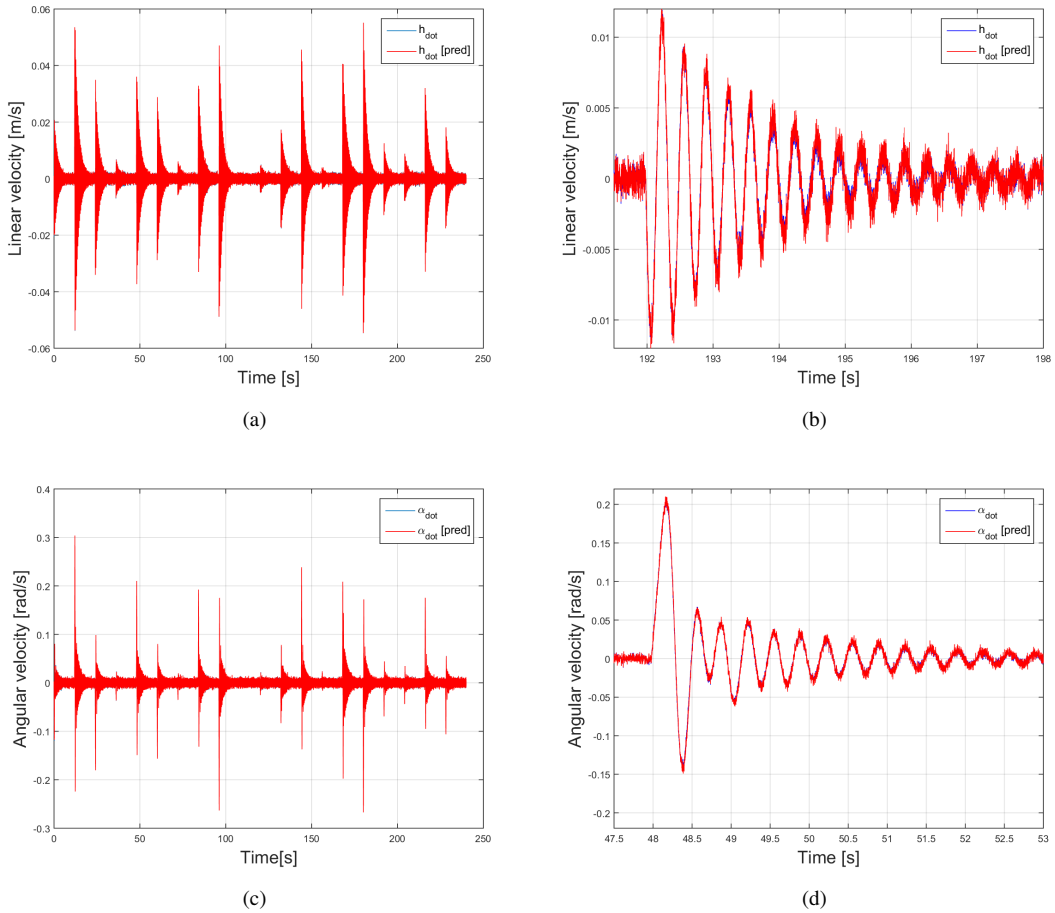

Figure 6 – (a) Output prediction for the linear velocity, $\dot{h}(n)$, (b) enlarged time for linear velocity, (c) output prediction for the angular velocity, $\dot{\alpha}(n)$ and (d) enlarged time for angular velocity.

The parameters used for the system simulation are extracted from the relationship between discrete-time and continuous-time model (Kukreja, 2008). In order to prepare the method for future real applications considering the experimental data, the noise is modeled as a Gaussian distribution with covariance $\sigma^2_{\dot{h}} = 0.04 \times 10^{-5}$ and $\sigma^2_{\dot{\alpha}} = 0.12 \times 10^{-4}$. The signal to noise ratio is 99.51 dB and 37.60 dB for the outputs $\dot{h}(n)$ e $\dot{\alpha}(n)$, respectively.

The process is excited by the angular displacement of the control surface β, with an aleatory signal having constant levels of 12 s each as depicted in Figure 5. The ELS procedure is repeated until iteration $k = 10$ and the identified parameters is presented in the Table 2.

To present the model output predictions, by convenience, the same data set is used for identification and validation.

The identification data corresponding to $2/3$ of the complete data set. The Figure 6 shows the output predictions of the identified model. From the identified discrete-time model parameters is possible to return to the continuous-time model. The identified stiffness parameters are present in the Table 3.

Table 3 – Parameters of the nonlinear stiffness.

Parameter	Value	Identified
k_{α_0}	3	2.99
k_{α_1}	-30	-30.24
k_{α_2}	6600	6592.35
k_{α_3}	-21000	-20325.51
k_{α_4}	48000	35672.42

The identified parameters of the nonlinear torsional stiffness are also suitable to represent the static nonlinearity present on the system dynamics. Although the parameter k_{α_4} has a very different value in comparison with the true one, the nonlinearity is in the range of interest, between the operational limits for the pitch angle, around 1.5 deg. The Figure 7 is obtained with simulated of continuous-time model. The static nonlinear behavior is well captured by the model. The nonlinearity of this system is assumed as symmetric.

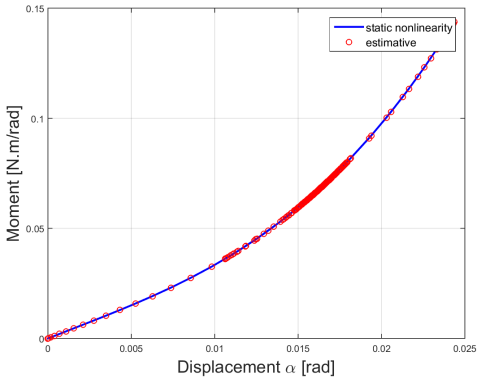

Figure 7 – A representation of the nonlinear behavior: moment as function of the angular displacement.

A STABILITY ANALYSIS

Stability analysis is important to map the regions where exists stable behavior for open loop operation. In cases where the instability occurs, the solution is the improvement of the control design in order to stabilize the system. One of the goals of this paper is the stability analysis using the identified model. The root locus and the damping factor diagram as function of the free stream velocity and the nonlinear stiffness are presented.

A continuous state-space model may be expressed as follows

$$\dot{\mathbf{x}}(t) = f_\mu[\mathbf{x}(t)] + g[\mathbf{x}(t)]\mu\beta \tag{11}$$

where the state-space variables are defined as

$$\{x_1(t),\, x_2(t),\, x_3(t),\, x_4(t)\}^T = \{h(t),\, \theta(t),\, \dot{h}(t),\, \dot{\theta}(t)\}^T \tag{12}$$

and consequently their derivatives are

$$\{\dot{x}_1(t),\, \dot{x}_2(t),\, \dot{x}_3(t),\, \dot{x}_4(t)\}^T = \{\dot{h}(t),\, \dot{\theta}(t),\, \ddot{h}(t),\, \ddot{\theta}(t)\}^T \tag{13}$$

Therefore the dynamic equation may be written as Equation 14. Note that the term $f_\mu(\mathbf{x})$ depends of the nonlinearity and will compound the Jacobian matrix. The control surface angle is null for the stability analysis.

$$\begin{Bmatrix} \dot{x}_1(t) \\ \dot{x}_2(t) \\ \dot{x}_3(t) \\ \dot{x}_4(t) \end{Bmatrix} = \begin{bmatrix} 0 & 0 & 1 & 0 \\ 0 & 0 & 0 & 1 \\ -k_1 & -[k_2\mu + pk_{x_2}(x_2(t))] & -c_1 & -c_2 \\ -k_3 & -[k_4\mu + qk_{x_2}(x_2(t))] & -c_3 & -c_4 \end{bmatrix} \begin{Bmatrix} x_1(t) \\ x_2(t) \\ x_3(t) \\ x_4(t) \end{Bmatrix} + \begin{bmatrix} 0 \\ 0 \\ g_3 \\ g_4 \end{bmatrix} \mu\beta \tag{14}$$

It can be observed that the term $k_{x_2}(x_2)$ is $k_\alpha(\alpha)$ and due the nonlinearity it is necessary to calculate the Jacobian matrix for evaluating the eigenvalues. Therefore the Jacobian matrix is given by

$$\mathbf{J} = \begin{bmatrix} 0 & 0 & 1 & 0 \\ 0 & 0 & 0 & 1 \\ -k_1 & -[k_2\mu + p(k_{\alpha 0} + k_{\alpha 1}\alpha(t) + k_{\alpha 2}\alpha(t)^2) + k_{\alpha 3}\alpha(t)^3] & -c_1 & -c_2 \\ -k_3 & -[k_4\mu + q(k_{\alpha 0} + k_{\alpha 1}\alpha(t) + k_{\alpha 2}\alpha(t)^2) + k_{\alpha 3}\alpha(t)^3] & -c_3 & -c_4 \end{bmatrix}_{|\alpha=\alpha_{op}} \tag{15}$$

It is possible verify the eigenvalues of the Jacobian matrix depends merely on the state values α. For this system the origin is a equilibrium point, therefore, the Figure 8 (a) shows the root locus for $\dot{\mathbf{x}} = \{0,0,0,0\}^T$.

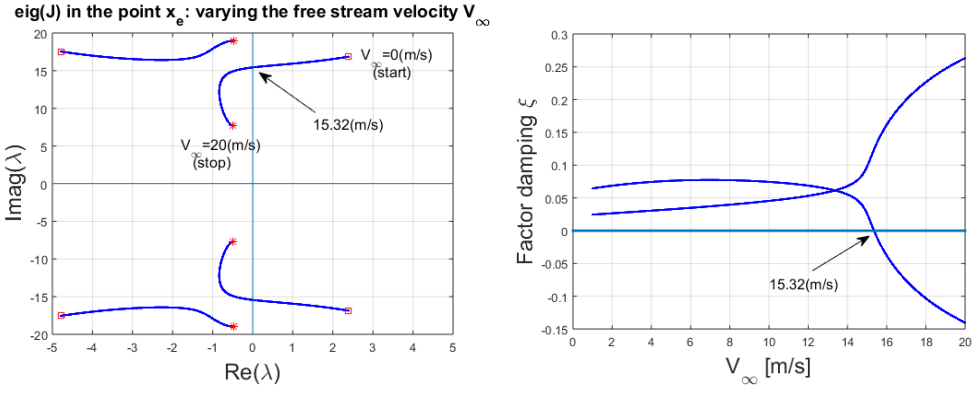

(a) (b)

Figure 8 – (a) Root locus for the free stream velocity variation considering the equilibrium point and (b) damping factor as functions of the free stream velocity.

From Figure 8(a), it can be seen that the instability occurs when the eigenvalue results cross the imaginary axis. This occurs for free stream velocity around 15.32 m/s, as shown in the Figure 8(b). In the instability region starts a LCO and the natural frequency of oscillation varies according to the angular displacement, because of the nonlinearity effects $k_\alpha(\alpha)$.

Influence of the pitch angle

According to equations of motion it is possible to verify that the nonlinearity affects the stability when a negative damping factor occurs, resulting in unstable behavior. The system becomes unstable due to the nonlinearity as shown in Figure 9. The figure is obtained varying the system operation point (named x_{op}). In this case, the angular displacement sweep occurred because the torsional stiffness is a function of the α values.

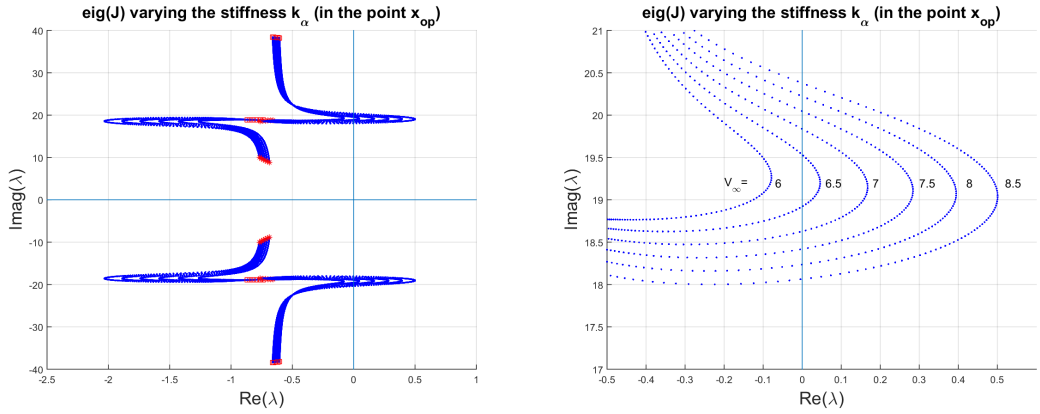

(a) (b)

Figure 9 – (a) Root locus for variation in nonlinear stiffness considering six free stream velocities and (b) enlarged region.

The Figure 9 shows six curves from the left to the right, each one corresponding to a free stream velocity of the range $\{6;6.5;7;7.5;8;8.5\}$ in m/s. The angular displacement is varying from 0 rad to 0.07 rad. Note that for reduced values of the free stream velocity, below 7 m/s, the nonlinearity does not affect the system stability. Above this value, the system is unstable depending on the angular displacement α of the operation point.

The root locus considering the free stream velocity of 8 m/s with the stiffness varying approximately from 0 Nm/rad to 27.07 Nm/rad is shown in Figure 11. It is observed in Figure 10(a) the region of instability for stiffness varying from 6.11 Nm/rad to 8.56 Nm/rad. Through several simulations it is possible to note that the LCO frequency increases as the stiffness rises, considering the stability region.

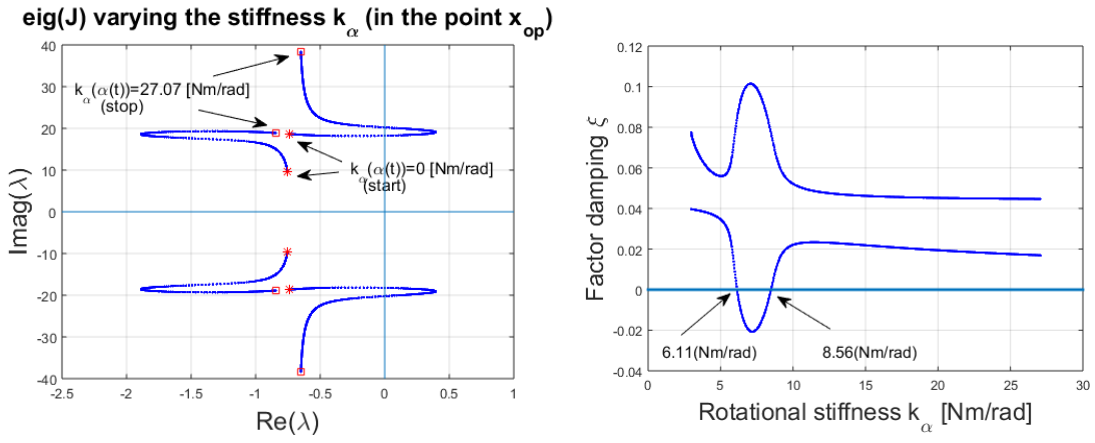

(a) (b)

Figure 10 – (a) Root locus for $V_\infty = 8\ m/s$ varying α between $0\ rad$ and $0.07\ rad$, (b) damping factor as function of a nonlinear stiffness.

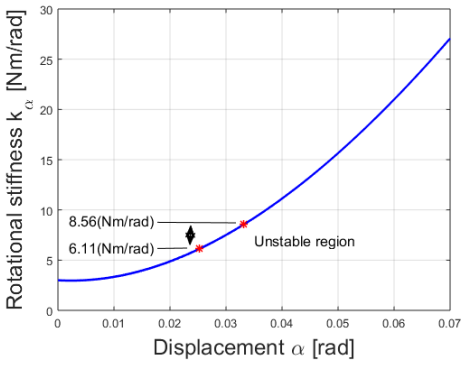

(a)

Figure 11 – Stiffness k_α versus angular displacement α.

CONCLUSION

The nonlinear identification applied to an aeroelastic pitch-plunge system is proposed using polynomial NARMAX model. A signal with pseudo-random sequence is used to excite the entire dynamic system. The polynomial NARMAX model is obtained using the extended least square estimator (ELS) to obtain unbiased estimation even with colored noise in measures.

The output predictions and an estimation of the static nonlinearity is presented in order to validate the identified model. The estimates converges quite quickly within ten iterations. The nonlinear identification results in a suitable nonlinear torsional stiffness. The proposed analysis is validated to be applied with the experimental data from the aeroelastic system. Also, the identified system serves to the stability analysis and the control system design with nonlinear approach.

From the stability analysis, the mapping of the unstable regions is outlined based on the eigenvalues of the Jacobian matrix. It concludes that the nonlinearity can lead the system to be dynamically unstable. The aeroelastic system is stable for velocity less than $V_\infty = 15.32\ m/s$ even with the nonlinearity. On the other hand, the system becomes unstable with the increase of the pitch angle and the free stream velocity. It is assumed an excursion of control surface with maximum angle of 15 deg, positive or negative, for normal operational in flight, but larger angles are tested for the identification process. In this work, the system is excited by the control surface from $-30\ deg$ to $30\ deg$. The root-locus is outlined for angular displacement between $0\ rad$ and $0.07\ rad$ corresponding to maximum angular displacement of $4.01\ deg$. The system operating in the unstable region can return to stable region by the action of the control surface leading on eigenvalues crossing the imaginary axis and returning to the left plane.

ACKNOWLEDGMENTS

This research has been financially supported by the MCT/CNPq/FAPEMIG National Institute of Science and Technology on Smart Structures in Engineering, grant no.574001/2008-5.

REFERENCES

Aguirre, L.A, 2007, introdução a identificação de sistemas: técnicas lineares e não-lineares , Ed. UMFG, 730 p.

Abdelkefi, A., Vasconcellos, R., Marques, F.D. and Hajj, M.R., 2012, Modeling and identification of freeplay nonlinear-

ity, Journal of Sound and Vibration, Vol. 331, pp. 1898-1907.
Billings, S.A., 2013, Nonlinear system identification: NARMAX methods in the time, frequency, and spatio-temporal domains, United Kingdom, Ed. Wiley, 574 p.
Dowell, E. 1989, A modern course in aeroelasticity, Ed. Springer, 575 p.
Farmer, M.G., 1982, A two-degree-of-freedom flutter mount system with low damping for testing rigid wings at different angles of attack, NASA Technical Memorandum.
Ko, J., Kurdila, A.J. and Strganac, T.W., 1997, Nonlinear dynamics and control for a structurally nonlinear aeroelastic system, AIAA , 13 p.
Kukreja, S.L., 2008, Nonlinear system identification for aeroelastic systems with application to experimental data, NASA Technical Memorandum.
Li, D., Guo, S. and Xiang, J., Aeroelastic dynamic response and control of an airfoil section with control surface nonlinearities, Journal of Sound and Vibration, Vol. 329, pp. 4756-4771.
Obeid, S., Jha, R. and Ahmadi, G. , 2012, Closed-loop feedback control of flow over a flapped airfoil at high angles of attack using identified NARMAX model, Proceedings of the ASME 2012 Fluids Engineering Summer Meeting.
O'Neil, T., 1996a, Nonlinear aeroelastic response - Analyses and experiments, AIAA Meeting Papers on Disc, Paper 96-0014.
O'Neil, T., Gilliatt, H. and Strganac, T.W., 1996b, Investigations of aeroelastic response for a system with continuous structural nonlinearities, AIAA Meeting Papers on Disc, Paper 96-1390.
O'Neil, T. and Strganac, T.W., 1998, Aeroelastic response of a rigid wing supported by nonlinear springs, Journal of Aircraft, Vol. 35, No. 4, pp. 616-622.
Popescu, C., Wong, Y. and Lee, B., 2005, System identification for nonlinear aeroelastic models, Proceedings of the 46th AIAA/ASME.
Shukla, H., 2016, Nonlinear Analysis and Control of Aeroelastic Systems.
Strganac, T.W., Ko, J. and Thompson, D.E., 2000, Identification and control of limit cycle oscillations in aeroelastic systems. Journal of Guidance, Control, and Dynamics, Vol. 23, No. 6, pp. 1127-1133.
Xu, X., Gao, Y. and Zhang, W., 2015, Aeroelastic dynamic response and control of an aeroelastic system with hysteresis nonlinearities, Journal of Control Science and Engineering, 10 p.

RESPONSIBILITY NOTICE

The authors are the only responsible for the material included in this paper.